AFRL-SR-BL-TR-99-

0865

# REPORT DOCUMENTATION PAGE

*Form Approved*
*OMB No. 0704-0188*



| 1. AGENCY USE ONLY (*Leave Blank*) | 2. REPORT DATE | 3. REPORT TYPE AND DATES COVERED |
|---|---|---|
| | July 30, 1999 | Final Technical Report<br>1 Apr 96 to 31 Mar 99 |

**4. TITLE AND SUBTITLE**
Protein Markers of Chemical Exposure and Molecular Epidemiology

**5. FUNDING NUMBERS**
F49620-96-1-0156

**5. AUTHOR(S)**
Frank A. Witzmann

**7. PERFORMING ORGANIZATION NAME(S) AND ADDRESS(ES)**
Molecular Anatomy Laboratory, Dept. of Biology
Indiana University Purdue University – Columbus
4601 Central Avenue
Columbus IN 47203

**8. PERFORMING ORGANIZATION REPORT NUMBER**

**9. SPONSORING/MONITORING AGENCY NAME(S) AND ADDRESS(ES)**
AFOSR/NL
801 North Randolph Street, Room 732
Arlington VA 22203-1977

**10. SPONSORING/MONITORING AGENCY REPORT NUMBER**

**11. SUPPLEMENTARY NOTES**

**12a. DISTRIBUTION/AVAILABILITY STATEMENT**
Approval for public release; distribution is unlimited.

**12b. DISTRIBUTION CODE**

**13. ABSTRACT (Maximum 200 words)**

This final technical report describes the results of experiments that 1) explored, at the molecular level, the toxicity of lead in various exposure systems; 2) enabled the development a system of general and tissue-specific protein markers for lead in rabbits and rats that might be indicative of its effect in human toxicologic targets; 3) assessed the cellular expression of GST isoenzymes as protein markers of lead toxicity in rat kidney; and 4) investigated the suitability of tissue-slice in vitro toxicologic approaches by evaluating their patterns of protein expression and comparing them to patterns from whole tissues. High resolution large-scale two-dimensional polyacrylamide gel electrophoresis (2-DE) with computerized image analysis was used to map cell/tissue proteins of various lead targets. In the case of lead experiments, proteomics technology, e.g. mass spectrometric analysis of tryptic digests (peptide-mass fingerprinting) of selected proteins resolved by 2-DE , was used to identify altered proteins. Quantitative and qualitative assessments of toxic effect were made, individual protein data was compiled in annotated databases, and protein markers identified.

**14. SUBJECT TERMS**

**15. NO. OF PAGES** 29

**16. PRICE CODE**

| 17. SECURITY CLASSIFICATION OF REPORT | 18. SECURITY CLASSIFICATION OF THIS PAGE | 19. SECURITY CLASSIFICATION OF ABSTRACT | 20. LIMITATION OF ABSTRACT |
|---|---|---|---|
| UNCLASSIFIED | UNCLASSIFIED | UNCLASSIFIED | |

NSN 7540-01-280-5500
Standard Form 298 (Rev. 2-89)
Prescribed by ANSI Std. Z39-18 298-102

## TABLE OF CONTENTS

## Abstract

This final technical report describes the results of experiments that 1) explored, at the molecular level, the toxicity of lead in various exposure systems; 2) enabled the development a system of general and tissue-specific protein markers for lead in rabbits and rats that might be indicative of its effect in human toxicologic targets; 3) assessed the cellular expression of GST isoenzymes as protein markers of lead toxicity in rat kidney; and 4) investigated the suitability of tissue-slice *in vitro* toxicologic approaches by evaluating their patterns of protein expression and comparing them to patterns from whole tissues. High resolution large-scale two-dimensional polyacrylamide gel electrophoresis (2-DE) with computerized image analysis was used to map cell/tissue proteins of various lead targets. In the case of lead experiments, proteomics technology, e.g. mass spectrometric analysis of tryptic digests (peptide-mass fingerprinting) of selected proteins resolved by 2-DE , was used to identify altered proteins. Quantitative and qualitative assessments of toxic effect were made, individual protein data was compiled in annotated databases, and protein markers identified.

The animals used in this study were handled in accordance with the principles stated in the Guide for the Care and Use of Laboratory Animals, prepared by the Committee on Care and Use of Laboratory Animal Resources, National Research Council, DHHS, National Institute of Health Publication #86-23, 1985, and the Animal Welfare Act of 1966, as amended.

## INTRODUCTION

**Toxicity of lead in various exposure systems and development a system of general and tissue-specific protein markers.** As a result of lead exposure, the mammalian kidney, a primary target organ in the initial accumulation of absorbed lead [1], takes it up through glomerular filtration, tubular reabsorption, and a small fraction through direct absorption [2-5]. Lead-induced nephrotoxicity in workers and experimental animals is well-documented and characterized as decreased glomerular filtration rate and nephropathy of proximal tubules [6, 7].

In terms of lead induced pathological damage to myocardium of humans, few studies are available, but histological examination of individuals who died from lead poisoning revealed degenerative and inflammatory changes in the myocardium [8]. In rats, blood lead levels greater than 110 μg/dL have been reported to cause myocardial edema, myofibrillar fragmentation, dilitation of sarcoplasmic reticulum, and myocardial swelling [9]. Despite evidence in both humans and experimental animals that high levels of lead poisoning can damage the myocardium, it has not been established if low blood leads comparable to those that occur in an occupational setting can damage the heart. One reason for this is that animal studies usually investigate the effect of a particular dose and rarely associate effects with blood lead levels [8,10]. We used an experimental rabbit model with sustained blood levels comparable to those found in occupational settings (20-80 μg/dL). In conjunction with full-scale assessment of lead toxicity in these rabbits, we screened ventricular myocardium for modifications in protein expression that might be associated with elevated blood lead levels. This was accomplished using high-resolution, large-scale two-dimensional electrophoresis (2-DE) and computerized image analysis.

Like many organs with multiple functions, the kidney consists of distinctly specialized regions with physiologic heterogeneities. The kidney is also a major target of many xenobiotics as either a primary and/or secondary result of toxic exposure [11]. Because the cortex is the primary site of filtration and filtrate reabsorption and the medulla is the site of renal filtrate concentrating mechanisms, it's not surprising to find that the two regions are constitutively different [12,13] and that these regions are differentially susceptible to toxic exposure [14,15]. Examining the effect of xenobiotic exposure on the expression of whole kidney homogenate protein patterns, as we have done previously [16,17], may not accurately reflect potential regiospecific changes. This is particularly true if these protein alterations are regionally diametrical, and thus may actually minimize or mask one another and be overlooked in analyzing a whole tissue homogenate. This same principle can be applied to whole cell versus cell-compartment studies. Therefore, we (1) studied the extent to which regional cytosolic component of the renal proteome varies in normal rodents using 2-D electrophoresis (2-DE) and computerized protein pattern image analysis and (2) determined the identity of some of the proteins (whose expression differed significantly) either immunologically or by MALDI-MS and ES-MS/MS Sequence Tag identification.

This initial experiment thus serves as the foundation for rodent lead nephrotoxicity studies and other renal proteomics applications.

Indicative of regional renal physiologic differences, histologic examination and enzyme assays confirm that the renal cortex and medulla are constitutively and biochemically different [12] and that lead accumulation [18] and lead-induced damage predominates in the cortical proximal tubular epithelium [1,19]. While preferential susceptibility of the highly vascularized cortex to the effects of lead is clear, lead effects on the medulla remain unexplored. Thus, experiments were undertaken to investigate the extent to which lead exposure alters regional renal protein expression and to determine which, if any, regionally distinct protein markers indicative of lead's renotoxic mechanism might be detected in kidney cortical and medullary cytosols.

**Assessment of glutathione S-transferase (GST) isoenzyme expression.** GSTs are a family of detoxification isoenzymes that catalyze the conjugation of xenobiotics and their metabolites with reduced glutathione and thus constitute an important defense mechanism against chemical toxicity. Lead exposure in rats is known to induce $\pi$-class GST (GSTP1) in the liver and almost all GST isoforms in the kidney [20]. The cytosolic family of GSTs consists of several families ($\alpha$, $\mu$, $\pi$, $\sigma$ and $\theta$) with catalytically active GSTs formed as homo- and heterodimers from subunits within each family. GSTs detoxify a variety of electrophilic organic compounds [21-23] and undergo transcriptionally-mediated increases in activity in response to lead exposure, prior to the development of lead-induced pathology [19]. GSTs may thus provide a biomarker of toxicant exposure. In an effort to further characterize lead-mediated effects on GSTs, the objectives of this study were: (1) to determine the isoenzyme profile and tissue specificity of cytosolic GST expression in the rat kidney using two-dimensional protein mapping, (2) to determine the effect of lead exposure on the expression of cytosolic GSTs, in terms of abundance alterations and chemical changes in the proteins involved, and (3) to determine the effect of *in vivo* lead exposure on GST isoform expression in rat kidney cytosols and consequently evaluate their potential utility as markers of lead toxicity. These preliminary observations of GST response to lead exposure are important components of this development with broad potential application to a variety of target tissues.

**Suitability of the tissue-slice *in vitro* toxicologic approach.** Finally, while 2-DE can be implemented successfully in *in vivo* and *in vitro* toxicologic studies [24], the latter has generally involved the use of isolated cells (*i.e.* cell culture, etc.). Extrapolation of toxic effects from isolated cells to intact tissues and organisms is somewhat problematic. To overcome this technical deficiency, the refinement of the tissue-slice technique [25] has enabled laboratories to avoid whole animal studies while conducting multiple preparations (50-100/tissue donor) and exposures in an in vitro system that is anatomically complete and structurally correct, relatively inexpensive, and conducive to interspecies comparison. In this last phase of this investigation, the effect of 1,3-dinitrobenzene (DNB) and 1,3,5-trinitrobenzene (TNB) on bovine testicular 2-DE protein pattern was examined to assess the utility of using 2-DE in

combination with the tissue-slice technique. 1,3-DNB and 1,3,5-TNB are formed in the manufacture of TNT, can be recovered from the wastewater effluent from TNT manufacture, and are themselves used as explosives. Additionally, DNB is used in the manufacture of dyes and in the synthesis of plastics. In rats, TNB (degradation products of trinitrotoluene) causes sperm depletion and seminiferous tubular degeneration [26]. In bovine testis slices exposed under conditions identical to those described in this report, TNB caused dose-related inhibition of protein synthesis, depletion of cellular K+, and cellular degeneration [27]. To describe their effects from a rather unique perspective and to evaluate the combination of *in vitro* tissue-slice exposures with 2-DE, the analysis of TNB- and DNB-induced protein pattern alterations was undertaken.

## MATERIALS AND METHODS

**Reagents.** Ultrapure electrophoretic reagents were obtained from Bio-Rad Inc. (Richmond, CA), Sigma Chemical Co. (St. Louis, MO), BDH (Poole, UK) and National Diagnostics (Atlanta, GA). Sequence grade trypsin was obtained from Roche Molecular Biochemicals (Indianapolis, IN). CHAPS (3-[(3-Cholamidopropyl)-dimethylammonio]-1-propanesulfonate) and dithiothreitol were obtained from CALBIOCHEM (La Jolla, CA) and N-isopropyl iodoacetamide from Molecular Probes (Eugene, OR). All other chemicals used were reagent grade. Hsc70, hsp70, and hsp90 antibodies were obtained from StressGen (Vancouver, BC), calbindin and calcineurin antibodies from Sigma Chemical Co. (St. Louis, MO), and anti-glutathione S-transferase P1 from Biotrin (Dublin, Ireland).

**Animals and treatments - Rabbit studies.** Sexually mature Dutch Belted rabbits (approximately 6-7 months old, 2 kg) were obtained from Hazelton Research Products (Aberdeen, MD). They were individually housed at NIOSH in Cincinnati OH, an AAALAC approved animal facility, in stainless steel (25" x 20" x 16") cages as required by the current USDA guidelines. A 12 hr light/dark cycle was maintained. Each rabbit was fed certified High Fiber Purina (#5325) rabbit chow (limited to 125 grams/day) and water *ad libitum*. Trace analysis including lead and pesticides were conducted on food and water. Lead treatment consisted of a 5-week pre-dosing period and a 15-week dosing period. The rabbits were randomized into a control and three dose groups (n = 15/group). A 5-week period was allowed to stabilize blood levels into the targeted ranges of 20, 40, and 80 μg/dl. Once target blood levels were obtained, each rabbit was placed on a maintenance dose regimen. Lead was administered as a lead acetate (PbAc) solution in sterile 5% dextrose via subcutaneous injection. The controls were given a subcutaneous injection of 5% dextrose. Each rabbit was given 3 ml of the loading dose solution three times per week during study weeks 6-10. Animals were dosed on a mg/kg basis as follows: 260, 360, or 1300 μg/kg lead to achieve targeted blood levels of 20, 40 or 80 μg/dL. Following the loading dose period, rabbits were then placed on a maintenance dose solutions during study weeks 11-20. The concentration of the maintenance dose solution administered was calculated using the previous week

blood lead value as a percentage of the expected dose. Animals were injected intravenously with 1250 IU heparin sodium via the marginal ear vein at least 20 minutes prior to sacrifice. Animals were weighed, then sacrificed by overdose with a concentrated solution of sodium pentobarbital (approximately 75 mg/kg) via the marginal ear vein, kidneys removed and frozen at -70°C. The thoracic cavity was opened, the heart was excised, and rinsed in iced Hank's Balanced Salts solution (Sigma Chemical Company, St. Louis, MO) within 2 minutes of injection of sodium pentobarbital. The whole heart was blotted dry with absorbent tissue and weighed. The atria were trimmed away, and the heart dissected along the septal insertion. The left ventricle was dissected into four pieces and stored at -70°C.

**Animals and treatments - Rat studies.** Sprague-Dawley male rats were bred and housed in the University of Wisconsin's Waisman Center animal care facility and given access to Tekland Rodent Blocks and water *ad libitum*. Eight-week-old rats, housed 4 per cage, were injected with lead acetate (114 mg/kg, 3 consecutive daily intraperitoneal (i.p.) injections; controls received physiological saline injections, i.p.). Rats were sacrificed on day 4 by $CO_2$ asphyxiation. Kidneys were decapsulated, and renal cortex and medulla were dissected. Each tissue was homogenized in 5 volumes of ice-cold 20 mM Tris-HCl, pH 7.8, 2 mM EGTA, 10 mM EDTA, 2 mM DTT. Cell fractions were prepared by differential centrifugation [28]. Protein concentration was determined by Bradford's [29] method.

**Preparation and incubation of testis-slices.** Bovine testicles were donated by Landes Meats, Inc., Dayton OH. Warm and cold ischemic times were 10 and 50 min, respectively. The tunic was stripped from each of 2 testicles studied and the tissue was cored (8 mm) and sliced (300 μm) in ice-cold Sacks buffer using a Brendel/Vitron slicer [30]. Slices were incubated using teflon/vitron/titanium rollers and a dynamic organ culture incubator as described previously [31]. Slices were placed on rollers, loaded into glass scintillation vials along with Waymouth's medium (1.7 mL/vial) supplemented with fetal calf serum, gentamicin (84 μg/mL), L-glutamine (3.5 mg/mL) and sodium bicarbonate (2.4 mg/mL), and pre-incubated for 30 min prior to exposure. TNB or DNB was added to the medium (dissolved in 50 μL ethane-1,2-dimethane sulfonate, DMSO) prior to inserting the slice and roller; exposures conducted at 100, 500, and 1000 mM for either 2, 4 or 6 hr (n=3 at each dose) along with DMSO controls (n=3 at each duration). Five naïve controls were studied as well as 3 incubated control slices at each duration. Incubation temperature was 34°C at an atmosphere of $O_2/CO_2$ (95/5). TNB and DNB incubations were conducted on different days using slices obtained from 2 different cattle. Control slices obtained from each testis were run and their results pooled.

**Sample preparation.** A 250 mg piece of each kidney and 500 mg piece ventricle of was sectioned (coronally) at or near the cortico-medullary boundary such that each sample was composed primarily of renal cortical cells. These samples were minced, ground-glass homogenized, solubilized in 2 ml of a lysis buffer (pH 9.5) containing 9 M urea, 4% CHAPS, 1% DTT (dithiothreitol) and 2% ampholytes (pH 8 - 10.5), and stored at -70°C until 2-DE.

All cell fractions (cytosol, microsomes, mitochondria, and nuclei) were solubilized by the addition of 1 volume of the lysis buffer described above.

Testis slices were solubilized in 8 volumes (175µl) of the lysis buffer in a 2 mL conical tube using 4 X 3 sec bursts of moderate sonication.

**2-DE & Image Analysis.** Sample proteins were resolved by 2-DE using a 20 x 25 cm 2-DE gel system (20 gels per run) [32]. Approximately 175 µg were applied to each isoelectric focusing (IEF) gel tube; gels were run for 25,000 volt-hours using a progressively increasing voltage protocol. A computer-controlled gradient casting system was used to prepare second dimension SDS gradient slab gels (11 to 17%T). First dimension IEF tube gels were loaded directly onto the slab gels without equilibration. Second dimension slab gels were run at 8°C for 18 h at 160V and then stained for 96 h using a colloidal Coomassie Blue G-250 procedure [33]. Stained gels were optically scanned at 121 micron resolution using a CCD scanner, and images were processed as described [24]. Groupwise statistical comparisons were made to screen for protein alterations (Student t-test). Charge modification index (CMI), calculated as described [34], is a numerical description of the overall average number of charges added per protein molecule and is thus an excellent estimate of the degree to which a protein is chemically (i.e. post-translationally) modified.

**Protein digestion.** Identical protein spots from 1-4 gels were excised manually, pooled, and then processed automatically using the DigestPro robot (ABiMED, Germany) [35]. The gel pieces were washed with 25 mM ammonium bicarbonate/50% acetonitrile followed by 100% acetonitrile. Proteins were reduced with 5 mM dithiothreitol in 25 mM ammonium bicarbonate for 30 minutes at 60°C, then alkylated with 10 mM iodoacetamide in 25 mM ammonium bicarbonate for 15 minutes at room temperature. Excess reagents were removed, and the gel pieces were rinsed with acetonitrile and dried under a stream of nitrogen. Proteins were digested overnight at 37°C in a total volume of 40 µl using Promega sequence grade, modified trypsin at a final concentration of 26 ng/µl in 30 mM ammonium bicarbonate/0.005% SDS [36]. Peptides were eluted at 37°C with 50 mM ammonium bicarbonate/60% acetonitrile, 0.1% trifluoroacetic acid/60% acetonitrile, and 100% acetonitrile for a final extraction volume of 240 µl.

**Matrix-assisted laser desorption mass spectrometric (MALDI) protein identification.** The resulting tryptic peptides were analyzed directly by MALDI after loading 5-10% aliquots of the digestion solutions onto thin film surfaces of α-cyano-4-hydroxycinnamic acid/nitrocellulose prepared by the fast evaporation method [37]. All mass spectrometry experiments were carried out on a PerSeptive Biosystems, Inc. (Framingham, MA 01701) Voyager DE-STR equipped with a N2 laser (337 nm, 3 ns pulse width, 20 Hz repetition rate). The mass spectra were acquired in the reflectron mode with delayed extraction. Internal mass calibration was performed with low-mass peptide standards, and mass-measurement accuracy was typically ±0.05 Da. The measured (MALDI) tryptic peptide masses were

used as inputs to search the NCBInr5.13.99 database containing 376,473 protein sequences. All searches were carried out using the Protein Prospector software developed at UCSF (see P.R. Baker and K.R. Clauser, http://www.prospector.ucsf.edu). No restrictions were placed on the species of origin of the protein. The allowed protein molecular weight range was 1,000 to 150,000 Da. Isoelectric points were allowed to range from 3.0 to 10.0, and oxidation of Met was included as a side-reaction. Up to 1 missed tryptic cleavage was considered, and a mass accuracy of ±0.2 Da was used for all tryptic-mass searches. The number of tryptic peptides required for identification varied as a function of the quality of the MALDI mass spectra.

## RESULTS & DISCUSSION

**Toxicity of lead in rabbit ventricle and kidney.** An average of 808 individual myocardial proteins were resolved and matched to the master pattern per sample; 162 (~20%) of which had coefficients of variation <20%, a reasonable indication of relative protein pattern consistency. Figure 1 (Appendix A) illustrates the schematic representation of the 2-DE protein master-pattern of rabbit ventricle homogenate. A number of proteins were tentatively identified based on coordinate positions homologous to other established 2D patterns and are labeled on the map. ANOVAs were conducted to identify protein spot abundances altered by lead exposure. Despite variable expression of some protein spots, none of the protein abundances analyzed differed among the experimental groups ($P<0.001$). The ventricular myosin regulatory light chains MLC1 and MLC2 represent two prominent proteins easily recognizable on conventional 2-DE pattern. These provisionally identified proteins are resolved as variable charge microheterogeneities [38-40], presumably as a result of chemical modification by phosphorylation following synthesis [41,42]. Figures 2 and 3 (Appendix A) illustrate that protein abundance and post-translational modification (as indicated by CMI) of these myocardial proteins were unaffected by lead exposure. Similarly, the abundance of tentatively identified α-tropomyosin and the E1 component, β-subunit precursor, of pyruvate dehydrogenase (Figure 4, Appendix A) were unaffected by lead exposure.

The dosing procedure used in the present study produced stable blood levels at or near the three targeted blood levels. Therefore, the rabbit provided an ideal experimental animal model for assessing the concentration-dependent effects of lead at blood levels below 100 μg/dL. 2-DE analysis of myocardial proteins did not reveal any significant alterations in protein expression of ventricular myocardium. Although we failed to detect an effect of elevated blood lead on the rabbit myocardium using 2-DE, the present study represents, to our knowledge, the first presentation of a 2-DE, protein expression profile of rabbit ventricular myocardium. Compared to those published maps and 2-DE gel images accessible for comparison on the World Wide Web (The Human Myocardial 2-D Electrophoresis Protein Database [http://www.chemie.fu-berlin.de/user/pleiss/dhzb.html] and 2-DE Gel Protein Databases at Harefield [http://www.harefield.nthames.nhs.uk/nhli/protein], the pattern presented in Figure 1 is

remarkably similar. As with rodent and canine species, the proteins in rabbit myocardium with high relative abundance were MLC1 and MLC2, actin, and tropomyosin, which are typical of myofibrillar abundance in myocardium. Further development of this in vivo model, by conclusive protein identification and expansion of the pH gradient using first-dimension IPG separation, is planned.

The master pattern for rabbit kidney homogenate is shown in Figure 5 and displays the coordinate positions of those proteins significantly altered by lead exposure ($p<0.005$). The filled circles/ellipses, identified by master spot number (MSN), represent those proteins whose abundance either increased or decreased following lead exposure. The protein alterations detected in the various exposure groups showed a significant, dose-related lead effect. At $p<0.001$ only 2 protein spots are altered, and these are in the highest lead level group (80ug/dl). At $p<0.005$ protein changes again occur only in the 80 ug/dl group with the exception of one protein, MSN 299, which is altered in the 40 ug/dl level group. The dose-related nature of this renal effect is clearly demonstrated by the protein alterations compared by Student t-test at a low $\alpha$, $p<0.05$. As Table 1 shows, the number of proteins exhibiting a change in mean quantity at this $\alpha$ increases almost exponentially with treatment. Alterations are noted in all lead groups, but the number increases with level of lead (12, 25 and 102 proteins in 20, 40 & 80 ug/dl lead, respectively).

**Table 1** Statistical Analysis of Kidney Homogenates from Lead-Treated Rabbits

| | **Number protein spots [Blood Lead] (ug/dl)** | **Percent Matched Protein Spots** |
|---|---|---|
| Matched protein spots [a] | 1100 | – |
| CV <15% [b] | 200 | (18%) |
| p<0.001 (vs. control) [c] | 2 (80 ug/dl) | (0.18%) |
| p<0.005 | 1 (40 ug/dl) | (0.09%) |
| " | 14 (80 ug/dl) | (1.3%) |
| p<0.05 | 12 (20 ug/dl) | (1.1%) |
| " | 25 (40 ug/dl) | (2.3%) |
| " | 102 (80 ug/dl) | (9.3%) |

[a] Average number of kidney protein spots in the master reference pattern (Figure 5, Appendix A) reproducibly resolved and matched to the individual sample gel patterns in each group.
[b] Coefficient of variance
[c] Student's t-test

Putative GST proteins were induced by lead as was enzymatic activity as measured by thioether formation (nmoles CDNB/min-mg). Four proteins cross-reacted with anti-rat GSTP1 (pi class GST Yp) antibody, MSN 187, 201, 246 and 392 (data not shown). The sum of the 4 abundances in each sample gives total GSTP1 abundance. This figure parallels induced GST activity as determined in the same tissue samples (Figure 6, Appendix A). In contrast, tentative identification of stress proteins (hsc70, hsp70 and hsp90) based on homologous coordinate position as compared to kidney patterns from rodents revealed no change in abundance with lead exposure.

The physiological significance of the observed protein alterations in kidney cannot be accurately assessed until the altered proteins are identified. Of particular interest are MSN 446, which demonstrated

a mean dose-related increase in abundance, and MSN 395 and possible charge variant of MSN 395, which demonstrated a dose-related decrease. Additionally, MSN 187, 201, 246 and 392 were induced to a lesser extent. Based on their coordinate positions and immunoreactivity to rat anti-GSTP1, these proteins may be glutathione s-transferase (GSTP1) charge variants (Fig 6). This identification and induction corresponds with rodent studies (see next section). Further development of this *in vivo* model, by conclusive protein identification and expansion of the pH gradient using first-dimensional IPG separation, is planned. These studies will provide enhanced understanding at the biochemical level of the lead-induced toxic effect on the kidney and offer additional insight into the putative basis for lead nephrotoxicity in the exposed human.

**Assessment of regional differences in renal lead toxicity.** An average of 727 protein spots were resolved and matched to the cortex cytosol reference pattern (Fig. 7, Appendix B) and 716 in the medulla cytosol (Fig. 8, Appendix B). The abundance of 122 proteins differed significantly (P<.001) between the two regions, with 82 proteins higher in cortex and 40 higher in medulla. Of these, 30 proteins were found to be unique to one region or the other (26 in cortex and four in medulla). Absent from the control cortical pattern, but detectable in medulla, was aldose reductase, while sorbitol dehydrogenase was more abundant in cortex. Aflatoxin B1 aldehyde reductase, hsp90, GSTP1 native and (-2) subunits, and transferrin were all more abundant in normal medullary cytosol than cortex. Conversely, α2-microglobulin, argininosuccinate synthase, calcineurin, calbindin, GST (-1), and sorbitol dehydrogenase were more abundant in the cortex.

Lead exposure significantly (P<.001) altered the abundance of 78 proteins in the cortex (42 increased and 36 decreased) (Table 2, Appendix B) and 16 proteins in the medulla (10 increased and 6 decreased) (Table 3, Appendix B). Of the cortical proteins altered by lead exposure, 24 were rendered undetectable in the lead-exposed group while l5 previously undetectable proteins were observed. In the medulla, eight proteins seen in control rats were undetectable after lead exposure whereas three previously undetectable proteins appeared in the lead-exposed group.

Tables 2 and 3 include the identified proteins found in the two kidney regions while Table 4 (Appendix B) lists only the identified proteins, comparing the lead effect and indicating the method of identification for each. Notable comparative lead-induced alterations include major increases in aldose reductase, aflatoxin B1 aldehyde reductase, and transketolase; major declines in α2-microglobulin and in cortical argininosuccinate synthase but not medulla (where it was already significantly lower); cortical increase in hsp90 (but not medulla where it was already elevated); cortical decline in transferrin but not medulla; decreased sorbitol deydrogenase, calbindin and calcineurin in cortex not in medulla, where all were already significantly lower.

Cytosolic GSTP1 was resolved as 3 or 4 charge variants due to chemical charge modification of the native form [43]. The magnitude of this modification, calculated as CMI, is shown in Figure 9 (Appendix

B). CMI in cortex is greater than in medulla but was altered by lead only in the cortex. Total GSTP1 abundance (sum of individual charge variant abundances) was the same in cortex and medulla from untreated rats. Lead-exposure increased GSTP1 abundance in both regions and had a significantly preferential effect on cortical GSTP1 (3-fold increase) compared to medulla (2-fold).

Five principal findings arose from these experiments: 1) Thirty proteins were found to be unique to either renal cortex or medulla; 2) lead administration altered the expression of 10% of the detectable cortical proteins and 2% of the proteins detected in medulla; 3) lead administration caused almost an equal number of increases and decreases in specific cortical proteins; 4) the largest changes observed were in the abundances of α2-microglobulin (down ninety percent in cortex and not detectable in medulla), aldose reductase (detectable in cortex only following lead administration and increased more than 20-fold in medulla after lead administration), GSTP, which increased six-fold in cortex after lead treatment, and aflatoxin B1 aldehyde reductase (two-fold increase in both cortex and medulla); and 5) lead administration altered the post-translational modification of GSTP in renal cortex.

Among proteins that were detected in unexposed renal medulla but not renal cortex, was aldose reductase. This finding is consistent with a previous report that aldose reductase mRNA levels in cortex are only one percent of those in medulla [44]. The detection of aldose reductase only in the medulla is consistent with published enzymatic data and recognized osmotic conditions in that region of the kidney, where aldose reductase functions in the NADPH-dependent conversion of glucose to slowly diffusible sorbitol which maintains osmotic balance during antidiuresis [45]. Medullary cells are exposed to far greater extracellular osmotic pressure than the isotonic cortical region and increases in sorbitol production serve to maintain the cellular integrity of renal medulla. It has been shown that aldose reductase decreases during diuresis, while sorbitol dehydrogenase increases. During antidiuresis, aldose reductase increases, while sorbitol dehydrogenase activity remains low [46]. Two possible mechanisms for aldose reductase induction by lead are suggested by the literature. Studies of aldose reductase promoter regions have identified a tonicity-responsive element, which would account for induction under conditions of antidiuresis which would follow dehydration [47]. However, following lead treatment, aldose reductase abundance increased (and sorbitol dehydrogenase abundance decreased) to a greater extent in renal cortex than in medulla where the highest interstitial osmolarity normally occurs. Recent (unpublished) results from a separate study conducted in this laboratory indicate normal blood osmolarity in rodents exposed to lead as described here. It is thus unlikely that dehydration and increased cortical osmolarity underly the lead-associated alterations. An alternative explanation lies in a report that oxidative stress causes induction of aldose reductase in smooth muscle cells and that this confers protection against the cytotoxic effects of aldehyde products of lipid peroxidation [48]. This may also explain the significant induction of the chemoprotective aflatoxin B1 aldehyde reductase, aldose reductase's relative in the aldo-keto

reductase superfamily AKR1 [49]. Lead-related oxidative stress could thus account for reductase induction though we have no direct evidence to support this notion.

The impact of lead on cellular calcium homeostasis has been demonstrated repeatedly but is not completely understood. Our observation of the nearly two-fold decrease in levels of the calcium-binding protein calbindin and the calmodulin-dependent protein phosphatase calcineurin is similar to the inhibition by lead of 1,25-dihydroxyvitamin D3-stimulated synthesis of calcium-binding proteins in bone cells [50] and presumably reflects a perturbation of calcium homeostasis in the renal cortex.

An examination of protein alterations in other cell fractions prepared from kidney cortex revealed that lead affects were dominant in the cytosol as the previous results would suggest. This comparison is illustrated in Figure 10, Appendix B.

**Assessment of glutathione S-transferase (GST) isoenzyme expression.** The protein patterns of rat kidney cytosol were resolved, GST isoenzymes identified and the effect of lead exposure on GST abundance and charge modification determined. Figure 11 (Appendix C) illustrates the representative 2-DE protein pattern of Sprague-Dawley kidney cytosol from a lead-treated rat. As expected, among the more than 700 protein spots resolved, Western blotting and immunostaining with GSTP1 antibody revealed only GSTP1 in this carrier ampholyte range. Control cytosol patterns contained only two GSTP1 spots, the native form (pI ~7.3) and a single acidic charge variant (pI ~7.1) (Fig. 11). Lead exposure caused the appearance of two more negatively charged variants as shown in Figures 11 and 12a. Quantitation of total GSTP1 abundance (sum of individual charge variant abundances, Fig. 12a & b, Appendix C) and charge modification via CMI calculation confirmed the induction and chemical modification of GSTP1 (Figure 12c). Lead exposure was accompanied by a 2.5X increase in GSTP1 abundance and a nearly 2X increase in CMI. Though the nature of the charge shift has not yet been elucidated, 2-DE Western blots probed with anti-phosphotyrosine antibody (not shown) demonstrated that GSTP1's charge variation was not due to tyrosine phosphorylation. Other possibilities consistent with the data include deamidation of glutamine or asparagine residues [51] or the phosphorylation of serine or threonine residues [52].

The GST isoforms with pI > 7.5 were not detected on the conventional ISO-DALT patterns. These were resolved on NEPHGE-DALT gels as shown on Western blots in Figure 12d. As expected, GSTM1 was not detected in the control kidney cytosol whereas lead exposure greatly increased the abundance of GSTM1 as seen in Fig. 12d, Appendix C. The NEPHGE-DALT pattern also confirmed the induction in GSTP1 observed in the ISO-DALT patterns. The magnitude of these lead-induced GST subunit alterations are consistent with previous enzymatic and morphologic observations of triethyl-lead [1] and lead acetate [19] induction of kidney GST. Additionally, 2-DE mapping of kidney GST isoforms and the analysis of their individual responses to lead exposure adds new information to our understanding of lead toxicity and offers an important tool for its investigation. At the same time, these results raise new

questions regarding the chemical modification of GSTP1 and the effects of lead on other cellular proteins resolved.

**Assessment of the tissue-slice *in vitro* toxicologic approach.** Liver slices have been shown to remain minimally viable in dynamic culture for up to 120 hr [53]. In a previous report [27], $^{3}$H-leucine incorporation by testis slices was linear throughout a 24 hour period. In this same study, the TNB dose- and time-related depression of protein synthesis (as indicated by decreased $^{3}$H-leucine incorporation) in replicates of samples similar to those tested in this study verified the adverse effects of TNB exposure. Not surprisingly, the present observations of testis slice exposure to TNB and DNB were typified by detectable and quantifiable alterations in the expression of several unidentified proteins on 2-DE patterns while specific incubation or DMSO-vehicle effects on protein pattern were not detectable. Figure 14 illustrates the upregulation (P<.001) of 7 protein spots by TNB, and to a lesser extent DNB (MSN 161 and 451, only). Given the down-regulation of total protein synthesis by TNB, these observations may well relate to differential turnover rates for these proteins such that some proteins, whose degradation is slower, appear to be induced. Nevertheless, these protein alterations are substantial, relatively consistent, and warrant protein identification. Conversely, Figure 15 illustrates the significantly (P<.001) reduced abundance of 8 protein spots. As in Figure 13, the dominant effects were associated with TNB exposure. Only MSN 48 and 131 were significantly altered by DNB. The differential abundances may be attributed, once again, to the differential turnover rates of testis proteins. However, assuming accurate sample loading and, more importantly, the correction via scaling for differential loading [24] conducted on each sample, generalized protein synthesis effects are accounted for and the observed changes are related to intoxication. Again, identification of the protein spots will provide mechanistic relevance to these selective declines in abundance. In addition to documenting observable pattern alterations, another consideration central to the validation of this approach was substantiating the consistency of spot resolution. To analyze this aspect of the results, we calculated the coefficient of variation (CV) for each group and for the entire experiment (mean CV of all groups). Matched patterns possessing a reasonable number of protein spots with CV < 15% (around 20% of matched spots) are deemed consistently resolved and *vice versa*. CV data for testis slices as well as other tissues, from a variety of previous experiments conducted in our laboratory, are presented in Table 5. In ranking the various percentages

**Table 5. Consistency of Protein Spot Resolution: Coefficient of Variation**

| Sample Type | # of Matched Spots | # of Spots with CV < 15% | % of Spots with CV < 15% |
|---|---|---|---|
| bovine testis slices* | 979 | 214 | 26% |
| SD rat brain* (cerebrum) | 978 | 233 | 24% |
| F344 rat kidney* | 1139 | 225 | 20% |
| mouse liver* | 1104 | 206 | 19% |
| human liver slices | 998 | 192 | 19% |
| SD rat liver* | 1174 | 178 | 15% |
| F344 rat liver* | 1267 | 187 | 15% |
| SD rat serum* | 606 | 47 | 8% |
| human liver | 1005 | 32 | 3% |
| human plasma* | 590 | 12 | 2% |

$CV = \frac{SD}{mean} X\ 100$ ** in samples with multiple groups, values are average CV*

of matched protein spots with CV < 15%, it is clear that bovine testis slices were consistently resolved; better, in fact, than many freshly sampled whole tissue homogenate protein patterns. While this ranking is encouraging, it is not altogether surprising. Serial tissue sections cut from an individual tissue core should have significant homogeneity. Conversely, prior to their oxygenation, the testis samples were subjected to warm (time between animal death and testicular excision and placement on ice) and cold ischemia for 10 and 50 minutes, respectively. This treatment, prior to slicing, could have introduced some protein variability.

## CONCLUSION

We have detected, quantified, and statistically compared numerous regionally distinct proteins in rabbit kidney, ventricle, rat kidney cortical and medullary cytosols and established some of these proteins as markers indicative of lead toxicity. Many of these prominent proteins have been conclusively identified, confirming previous enzymatic observations of regional differences in renal protein expression, establishing new insights into the molecular heterogeneity characterizing structural and functional regions of the kidney, and suggesting regiospecific mechanisms of lead nephrotoxicity. Further investigation of these lead effects via additional systematic protein identification combined with a lead dose-response approach in all cell compartments and whole-tissue homogenates is underway.

We examined the combination of 2-DE analysis and *in vitro* chemical exposure of bovine testis slices, using protein pattern alterations and coefficient of variation as standards. Consistency of protein separation and detection, comparable to *in vivo* model systems, was achieved and structurally-specific chemically-induced protein alterations were documented. The results of this investigation demonstrate the potential toxicologic utility of combining in vitro tissue-slice technology with high-resolution 2-DE protein mapping. The consolidation of these two reliable methods offers a novel approach for toxicity screening and testing, reduces the use of laboratory animals, and reduces experimental cost.

Ongoing rodent tissue proteome analysis (including cell compartments) supported bu continued funding will extend these results and provide a unique framework within which to study toxicity of a JP-8 jet fuel.

## LITERATURE CITED

[1] Nolan, C.V., Shaikh, Z.A., *Toxicology*, 1992, 73, 127-146.
[2] Vostal, J. and Heller, J., *Environ. Res.*, 1968, 2, 1- 10.
[3] Vander, A.J., Taylor, D.L., Kalitis, K., Mouw, D.R., Victery, W., *Am. J. Physiol.*, 1977, 233, F532-538.
[4] Victery, W., Vander, A.J., Mouw, D.R., *Am. J. Physiol.*, 1979, 237, F398-407.
[5] Victery, W., Vander, A.J., Mouw, D.R., *Am. J. Physiol.*, 1979, 237, F408-414.
[6] Goyer, R.A., *Curr. Topics Pathol.*, 1971, 55, 147-176.

[7] Wedeen, R.P., Maesaka, J.K., Weiner, B., Lipat, G.A., Lyons, M.M., Vitale, L.F.
[8] Kopp, S.J., Barron, J.T., Tow, J.P., *Environ. Health Perspec.*, 1988, 78, 91-99.
[9] Asokan, S.K., *J. Lab. Clin. Med.*, 1974, 84, 20-25.
[10] Victery, W., *Environ. Health Perspec.*, 1988, 78, 71-76.
[11] Werner, M., Costa, M.J., Mitchell, L.G., Nayar, R., *Clin. Chim. Acta*, 1995, 237, 107-154.
[12] Jacobson, H.R., *Am. J. Physiol.*, 1981, 241, F203-218.
[13] Valtin, H., *Am. J. Physiol.*, 1977, 233, F491-501.
[14] Diamond, G.L., Zalups, R.K., *Toxicol. Pathol.*, 1998, 26, 92-103.
[15] Fowler, B.A., *Environ. Health Perspect.*, 1993, 100, 57-63.
[16] Witzmann, F., Clack, J., Fultz, C., Jarnot, B., *Electrophoresis*, 1995, 16, 451-459.
[17] Witzmann, F.A., Fultz, C.D., Lipscomb, J.C., *Electrophoresis*, 1996, 17, 198-202.
[18] Tarloff J.B., Goldstein R.S.in: Hogson, E., Levi, P.E., (Eds.), *Introduction to Biochemical Toxicology*, Appleton and Lange, Norwalk, Conn. 1994, pp. 519-546.
[19] Oberley, T.D., Friedman, A.L., Moser, R., Siegel, F.L., *Toxicol. Appl. Pharmacol.*, 1995, 131, 94-107.
[20] Daggett, D.A., Nuwaysir, E.F., Nelson, S.A., Wright, L.S., Kornguth, S.E., Siegel, F.L., *Toxicology* 1997, 117, 61-71.
[21] Ketterer, B., Meyer, B.J., Clark, A.G., in: Sies, H., Ketterer, B. (Eds.), *Glutathione Conjugation: Mechanism and Biological Significance*. Academic Press, London, 1988, pp. 73-135.
[22] Mannervik, B., Danielson, U.H., *CRC Crit. Rev. Biochem.*, 1988, 23, 283-337.
[23] Vos, R.M.E., Van Bladeren, P.J., *Chem. Biol. Interact.*, 1990, 75, 241-165.
[24] Anderson, N.L., Esquer-Blasco, R., Anderson, N.G., in: Tyson, C.A., Frazier, J.M. (Ed's.), *Methods in Toxicology Vol 1. Part B* In Vitro *Toxicity Indicators*, Academic Press, San Diego CA 1994, pp. 463-473.
[25] Krumdieck, C.L., DosSantos, J.E., Ho, K., *Anal. Biochem.*, 1983, 104, 118-123.
[26] Kinkead, E.R., Wolfe, R.E., Fleming, C.D., Caldwell, D.J., Miller, C.R., Marit G.B., *Toxicol. Indust. Health*, 1995, 11,309-23.
[27] Wyman, J.F., Grabau, J., Graeter, L., *ISSX Proceedings*, 1995, 8, 200.
[28] Tata, J.R. in: Birnie, G.D. (Ed.), *Subcellular Components*, Butterworths, London 1972, pp. 185-214.
[29] Bradford, M.M., *Anal. Biochem.*, 1976, 72, 248-254.
[30] Brendel, K., Fisher, R.L., Krumdieck C.L., Gandolfi, J., *Methods Toxicol.*, 1993, 1A, 222-230.
[31] Sipes, I.G., Fisher, R.L., Smith, P.F., Stine, E.R., Gandolfi, A.J., Brendel, K., *Arch. Toxicol. Suppl.*, 1987, 11, 20-33.
[32] Anderson, N.L., *Two-dimensional Electrophoresis: Operation of the ISO-DALT System*, 1991, Large Scale Biology Press, Washington DC.
[33] Neuhoff, V., Arnold, N., Taube, D,, Ehrhardt, W., *Electrophoresis*, 1988, 9, 255-262.
[34] Anderson, N.L., Copple, D.C., Bendele, R.A., Probst, G.S., Richardson, F.C., *Fundam. Appl. Toxicol.*, 1992, 18, 570-580.
[35] Houthaeve, T., Gausephol, H., Mann, M., Ashman, K., *FEBS Letters*, 1995, 376, 91-94.
[36] Arnott, D., O'Connell, K.L., King, K.L., Stults, J.T., *Anal. Biochem.*, 1998, 258, 1-18.
[37] Fink, A.L., *Physiol. Rev.*, 1999, 79, 425-449.
[38] Thiede, B., Otto, A., Zimny-Arndt, U., Muller, E.C., Jungblut, P., *Electrophoresis*,1996, 17, 588-599.
[39] Kovalyov, L.I., Shishkin, S.S., Efimochkin, A.S., Kovalyova, M.A., Ershova, E.S., Egorov, T.A., Musalyamov, A.K., *Electrophoresis*, 1995, 16, 1160-1169.
[40] Pleißner, K.-P., Regitz-Zagrosek, V., Weise, C., Neuss, M., Krudewagen, B., Soding, P., Buchner, K., Hucho, F., Hildebrandt, A., Fleck, E., *Electrophoresis*,1995, 16, 841-850.
[41] Westwood, S.A., Perry, S.V., *Biochem, J.*, 1981, 197, 185-193.
[42] Whalen, R.G., Ecob, M.S., *Clin. Chem.*, 1982, 28, 1036-1040.

[43] Witzmann, F.A., Daggett, D.A., Fultz, C.D., Nelson, S.A., Wright, L.S., Kornguth, S.B., Siegel, F.L., *Electrophoresis*, 1998, 19, 2491-2497
[44] Dorin, R.I., Shah, V.O., Kaplan, D.L., Vela, B.S. and Zager, P.G., *Diabetologia*, 1995, 38, 46-54.
[45] Sands, J.M. and Schrader, D.C., *J. Am. Soc. Nephrol.*, 1990, 1, 58-65.
[46] Martial, S., Price, S.R., and Sands, J.M., *J. Amer. Soc. Nephrol.*, 1995, 5, 1971-1978.
[47] Daoudal, S., Tournaire, C., Halere, A., Veyssiere, G. and Jean, C., *J. Biol. Chem.*, 1997, 272, 2615-2619.
[48] Spycher, S.E., Tabataba-Vakili, S., O'Donnell, V.B., Palomba, L. and Azzi, A., *FASEB J.*, 1997, 11, 181-188.
[49] Jez, J.M., Flynn, T.G. and Penning, T.M., *Biochem. Pharmacol.*, 1997, 54, 639-647.
[50] Pounds, J.G., *Neurotoxicology*, 1984, 5, 295-331.
[51] Funakoshi, S., Deutsch, H.F., *J. Biol. Chem.*, 1968, 243, 6474-6481.
[52] Bulavin, D.V., Karpishchenko, A.I., Gubanov, A.I., Reshetov, A.V., *Biokhimiia.*, 1996, 61, 1015-27.
[53] Parrish, A.R., Gandolfi, A.J., Brendel, K., *Life Sci.*, 1995, 57, 1887-1901.

**Personnel Supported by this grant:**

Frank A. Witzmann, Ph.D. Principal Investigator
Carla D. Fultz, B.S. Research Technician

**Collaborators:**

John Wyman
Manntech

Daniel A. Daggett, Lynda S. Wright, Steven E. Kornguth and Frank L. Siegel
University of Wisconsin

Ray Grant
Procter & Gamble Company

Mark Toraason and Helen Kanitz
NIOSH

**Publications:**

Witzmann, F.A., C.D. Fultz & J.F. Wyman. (1997). Two-dimensional electrophoresis of precision-cut testis slices: toxicologic application. Electrophoresis 18, 642-646.
Fultz, C.D. & F.A. Witzmann. (1997). Locating Western blotted and immunostained proteins within complex two-dimensional patterns. Analytical Biochemistry 251, 288-291.
Toraason, M., W. Moorman, P. Mathias, C. Fultz, & F. Witzmann. (1997). Two-dimensional electrophoretic analysis of myocardial proteins from lead-exposed rabbits. Electrophoresis 18, 2978-2982.
Witzmann, F.A., D.A. Daggett, C.D. Fultz, S. A. Nelson, L.S. Wright, S.E. Kornguth & F.L. Siegel. (1998). Glutathione s-transferases: 2-DE protein markers of lead exposure. Electrophoresis 19, 1332-1335.

Witzmann, F.A., C.D. Fultz, R.A. Grant, L.S. Wright, S.E. Kornguth & F.L. Siegel. (1998). Differential expression of cytosolic proteins in the rat kidney cortex and medulla: preliminary proteomics. Electrophoresis 19, 2491-2497.

Witzmann, F.A., C.D. Fultz, R.A. Grant, L.S. Wright, S.E. Kornguth & F.L. Siegel. (1999). Regional Protein Alterations In Rat Kidneys Induced By Lead Exposure. Electrophoresis 20, 943-951.

Kanitz, M.H., F. Witzmann, J.C. Clark, W.J. Moorman, and R.E. Savage. (1999). Alterations in rabbit kidney protein expression following lead exposure as analyzed by two dimensional gel electrophoresis. Electrophoresis (in press).

**Presentations:**

1,3,5-Trinitrobenzene toxicity in bovine testicular tissue-slices: two-dimensional electrophoretic analysis. Society of Toxicology Annual Meeting, Anaheim CA, 1996.

Two-dimensional Electrophoresis of Precision-cut Tissue Slices: Toxicologic Applications. From Genome to Proteome: 2nd Siena 2D Electrophoresis Meeting, Siena Italy, 1996.

Protein biomarkers of chemical exposure and molecular toxicity. Air Force Office of Scientific Research Predictive Toxicology Program Review, Fairborn OH, 1996.

Two-dimensional electrophoretic analysis of myocardial proteins from lead-exposed rabbits. Society of Toxicology Annual Meeting, Cincinnati OH, 1997.

Effect of lead acetate on glutathione S-transferase isoenzymes in Fischer 344 rats. Society of Toxicology Annual Meeting, Cincinnati OH, 1997.

Glutathione S-transferases: 2-DE protein markers of lead exposure. Electrophoresis '97 Meeting, Seattle WA, 1997.

Regional Protein Alterations In Rat Kidneys Induced By Lead Exposure. Society of Toxicology Annual Meeting, Seattle WA, 1998.

Renal Protein Markers of Lead Exposure. Society of Toxicology Annual Meeting, Seattle WA, 1998.

Tissue/Blood Biomarkers: Two-dimensional Protein Mapping. International Conference on the Environmental Health and Safety of Jet Fuel, San Antonio TX, 1998.

Applied Proteomics – Investigating the Nephrotoxicity of Lead. From Genome to Proteome: 3rd Siena 2D Electrophoresis Meeting, Siena, Italy 1998.

Proteomic Data: Potential Molecular Biodescriptors for Hierarchical QSAR. Molecular Descriptors and Their Applications in Structure-Property-Activity-Toxicity Relationships. Natural Resources Research Institute, University of Minnesota, Duluth MN, 1999.

**Transitions:**

Customer #1: Dr. Frank Siegel, University of Wisconsin Medical School, Madison WI

*Result:* Protein mapping of isoforms of glutathione-S-transferase and their response to lead and chromium intoxication

*Application:* Protein mapping studies will be used to assess human risk based on protein pattern alterations associated with genotoxic and nongenotoxic cellular effects of heavy metals.

Customer #2: Dr. N. Leigh Anderson, Large Scale Biology Corp., Rockville MD

*Result:* Identification of previously unidentified protein spots on 2DE protein maps of cells, tissues, and organs in various species and the addition of these data to the growing Tissue Effects Databases under development at LSB.

*Application:* LSB and its colleagues are building databases that describe how genes are regulated, and how this regulation changes in disease, after pharmacologic treatment and chemical exposure.

Customer #3: Dr. Ray Grant, The Procter & Gamble Company, Cincinnati OH
Result: Technical guidance regarding 2D protein separations in exchange for mass-spectrometric analysis and identification of proteins from AF studies.
Application: P & G is involved in proprietary drug development studies and is applying the large-scale 2DE process used in our studies to investigate protein effects.

Customer #4: Dr. John Strahler, NIH/Mich. State Univ. Mass Spec. Facility, E. Lansing MI
*Result:* Provided 2D gel protein-cutouts for the identification of post-translational modification of glutathione s-transferase by lead exposure.
*Application:* The NIH/MSU facility is developing methodology to routinely identify chemical modifications of proteins based on matrix-assisted laser desorption and tandem mass spectrometry.

# Appendix A

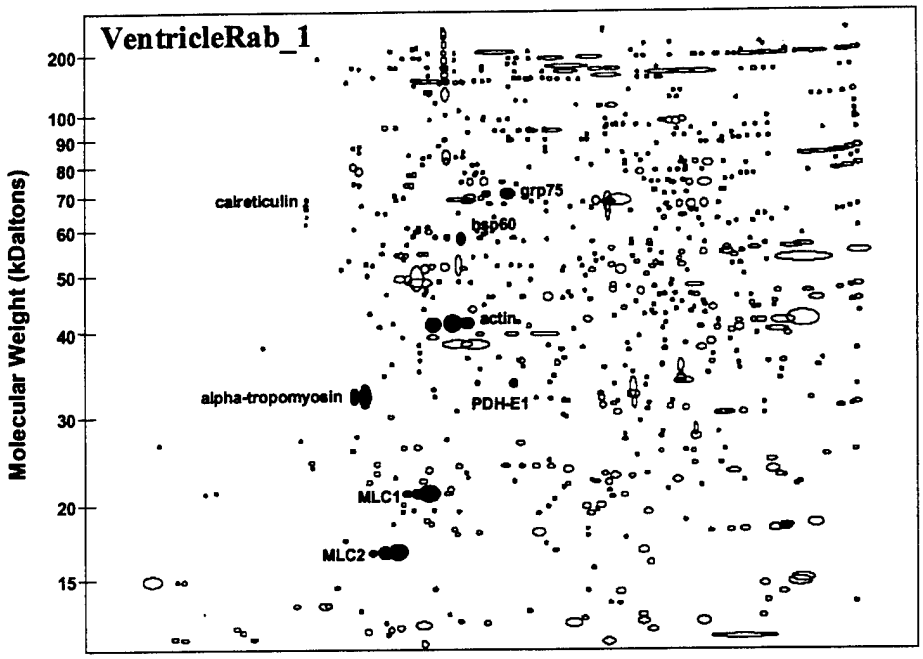


**Figure 1** Schematic map of the 2D protein master-pattern of rabbit ventricle homogenate. Acidic proteins are oriented to the left, basic to the right, low MW at the bottom, and high MW proteins toward the top. The horizontal dimension represents a pH gradient of 4-8. This pattern includes all proteins detected in all samples and is thus a composite, not necessarily representative of any one sample pattern. Each circle or ellipse represents either a distinct protein or alternate forms of the same protein. Each protein spot is also arbitrarily assigned a master spot number (MSN) establishing that protein's identity in the database for VentricleRab. The shaded spots are those identified by homologous position in other established patterns.

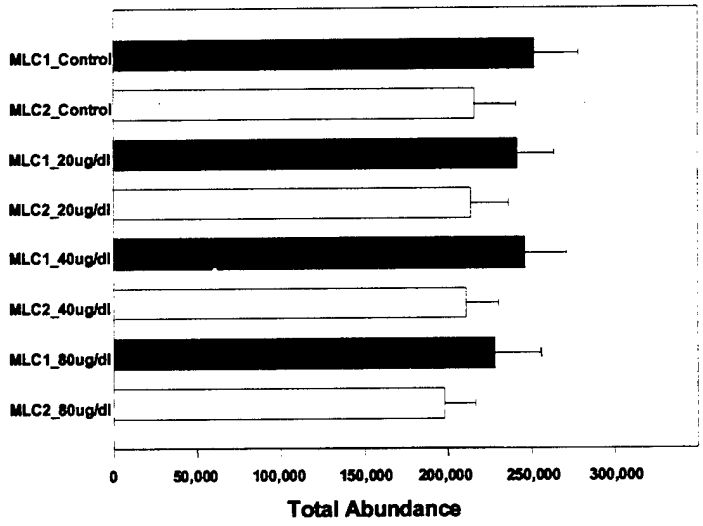


**Figure 2** Effect of lead exposure on myosin light chain charge variants. Lead exposure had no detectable effect on total abundance of the light chain spots. Data presented in this figure were used to calculate individual charge modification indices, an estimate of the level of post-translational modification, as shown in Fig. 3.

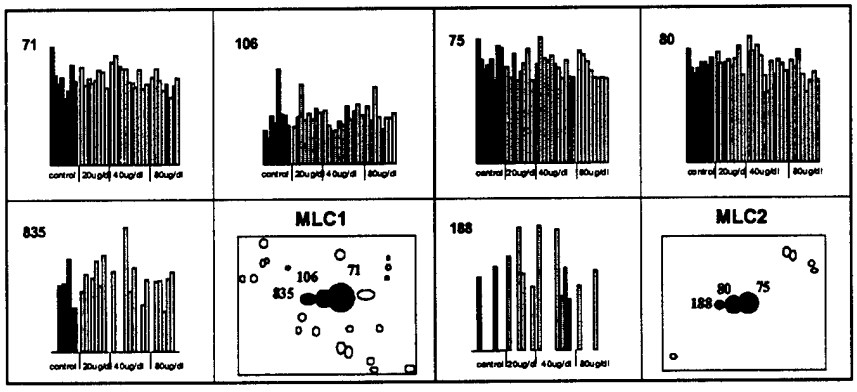


**Figure 3** Effect of lead exposure on myosin light chain charge modification index (CMI). CMI is a quantitative measure of the extent to which a protein is chemically (post-translationally) modified (i.e. phosphorylated, glycosylated, methylated or deaminated) and is calculated as described in the Methods. Lead had no effect on either light chain's CMI.

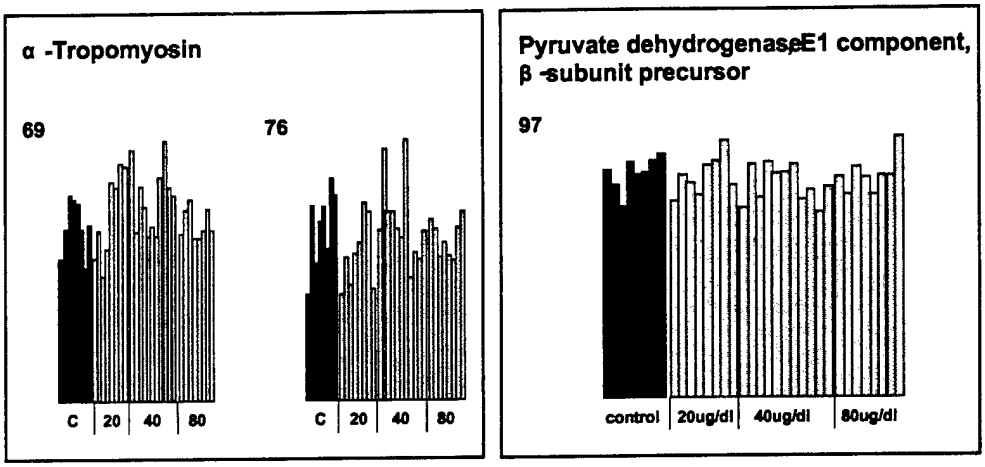


**Figure 4** Effect of lead exposure on two other tentatively identified myocardial proteins, α-tropomyosin (exists as two charge variants, MSN 69 and 76) and the E1 component, β-subunit precursor, of pyruvate dehydrogenase (MSN 97). These data illustrate a consistent pattern of protein abundances across the treatment groups where individual variations indicate a general lack of effect on myocardial proteins by these lead exposures.

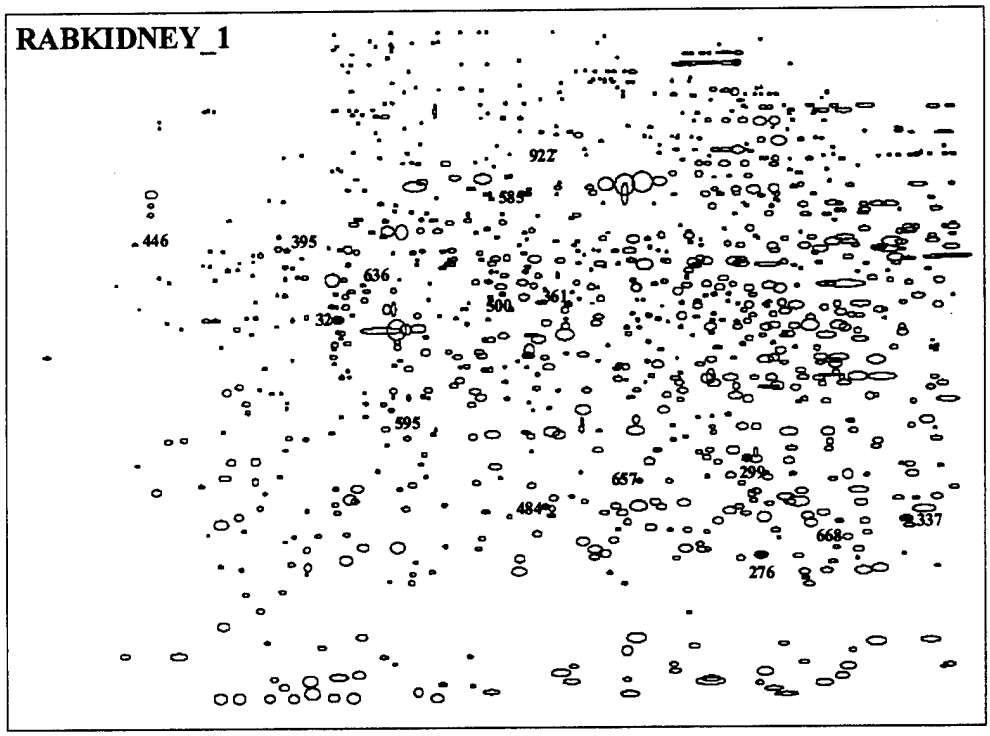


**Figure 5** 2-DE map of rabbit kidney master (reference) pattern containing all proteins resolved in this experiment. The horizontal dimension represents a pH gradient of approximately 4-7. High MW proteins are located nearer the top of the pattern, low MW nearer the bottom. The circles/ellipses shown in red and labeled by Master Spot Number (MSN) are those altered (P<.005) by lead exposure.

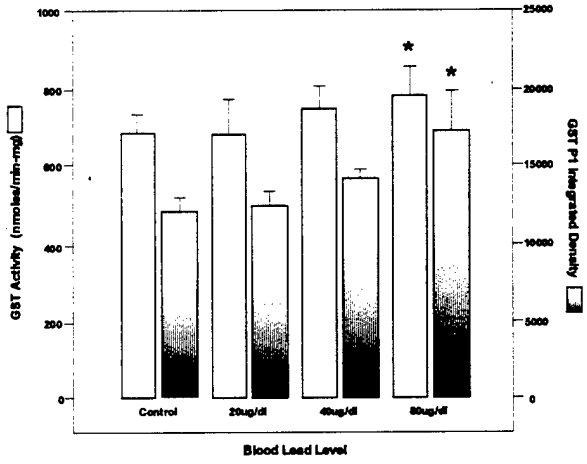


**Figure 6** The effect of lead exposure on total GST activity (as measured by thioether formation) and total putative GSTP1 abundance (sum of integrated densities). Values are means ± SE. *P<.05 following ANOVA.

## Appendix B

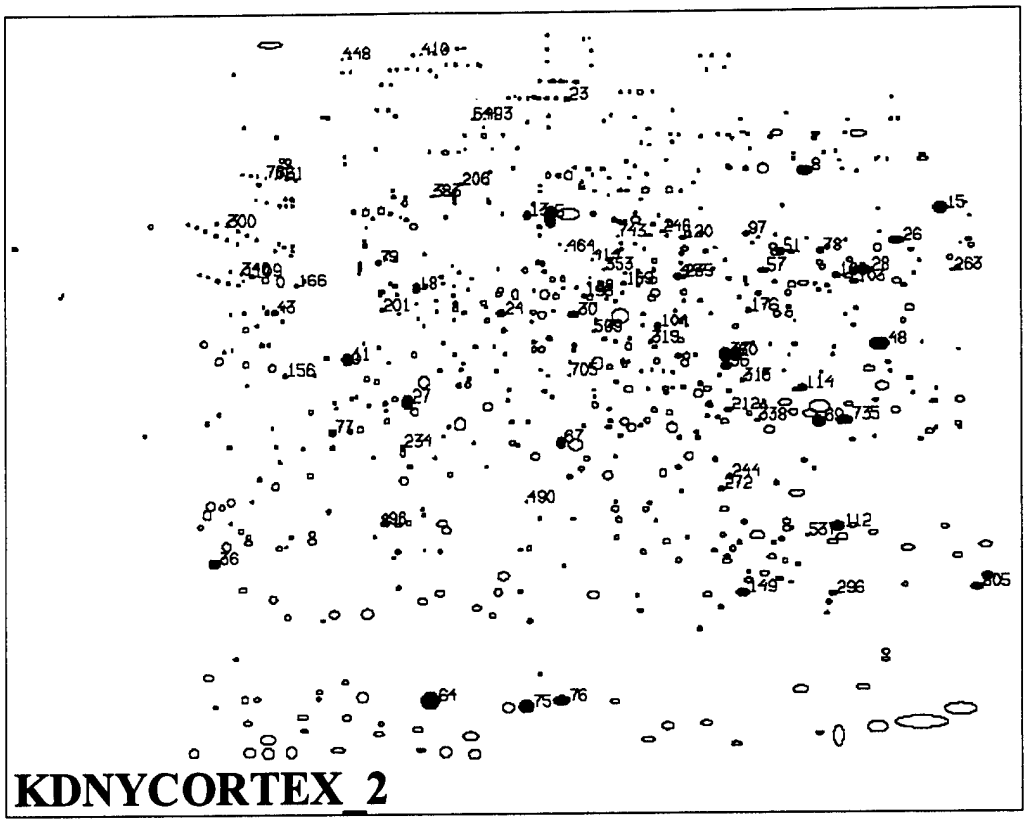


**Figure 7** 2-DE map of rat kidney cortex cytosol master pattern highlighting the coordinate positions and MSN of those proteins whose abundance was altered by lead acetate exposure (P<.001).

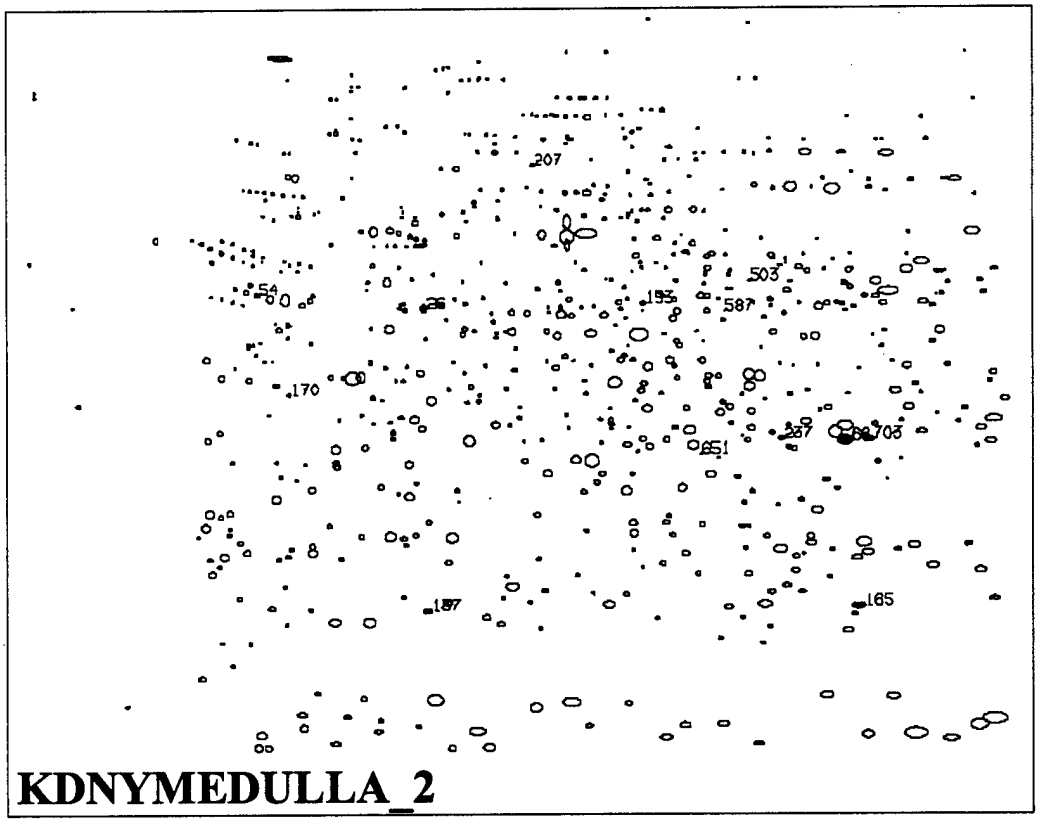


**Figure 8** 2-DE map of rat kidney medulla cytosol master pattern highlighting the coordinate positions and MSN of 13 proteins whose abundance was altered by lead acetate exposure (P<.001).

## Table 2. Rat kidney cortex cytosol proteins altered by lead exposure

| MSN[a] | ID | Mean Control Abundance | Mean Lead Abundance | PROB[b] | % of Control |
|---|---|---|---|---|---|
| 5 | | 78,810 | 57,250 | 0.009 | 73 |
| 8 | transferrin | 48,860 | 32,600 | 0.0005 | 67 |
| 11 | | 38,220 | 46,390 | 0.0002 | 121 |
| 13 | | 10,310 | 6,685 | 0.0009 | 65 |
| 15 | transketolase | 40,320 | 52,690 | 0.0008 | 131 |
| 18 | | 11,980 | 9,000 | 0.0006 | 75 |
| 21 | hsp90 | 4,857 | 7,548 | 0.008 | 155 |
| 23 | | 5,879 | 3,812 | 0.00007 | 65 |
| 24 | | 16,170 | 11,420 | 0.00008 | 71 |
| 26 | | 25,820 | 18,370 | 0.0001 | 71 |
| 27 | | 22,880 | 7,986 | 0.0003 | 35 |
| 28 | | 36,090 | 27,770 | 0.0002 | 77 |
| 30 | | 19,080 | 15,930 | 0.0008 | 83 |
| 36 | calbindin | 21,430 | 12,910 | 0.0007 | 60 |
| 37 | | 41,010 | 30,810 | 0.0002 | 75 |
| 43 | | 6,733 | 1,174 | 0.00002 | 17 |
| 44 | | 9,538 | 6,807 | 0.0003 | 71 |
| 48 | argininosuccinate synthase | 69,860 | 15,380 | 0.00002 | 22 |
| 51 | calcineurin | 8,703 | 3,340 | 0.0001 | 38 |
| 56 | | 22,800 | 18,290 | 0.0001 | 80 |
| 57 | | 9,309 | 7,164 | 0.001 | 77 |
| 60 | | 19,410 | 11,310 | 0.00009 | 58 |
| 64 | alpha-2 microglobulin | 69,570 | 5,977 | 0.00001 | 9 |
| 67 | | 17,270 | 23,150 | 0.0002 | 134 |
| 69 | aflatoxin B1 aldehyde reductase | 44,850 | 99,810 | 0.000002 | 223 |
| 75 | | 31,240 | 2,358 | 0.00005 | 8 |
| 76 | | 44,130 | 35,440 | 0.0003 | 80 |
| 77 | | 7,868 | 4,821 | 0.0004 | 61 |
| 78 | calcineurin | 7,718 | 5,503 | 0.0005 | 71 |
| 79 | | 4,134 | 7,536 | 0.0006 | 182 |
| 85 | alpha-2 microglobulin | 9,675 | - | NA | NA |
| 96 | | 8,858 | 14,850 | 0.00007 | 168 |
| 97 | | 5,111 | 4,435 | 0.001 | 87 |
| 99 | hsp90 | 2,140 | 3,173 | 0.03 | 148 |
| 103 | | 7,393 | 8,669 | 0.0009 | 117 |
| 104 | | 6,249 | 4,652 | 0.002 | 74 |
| 106 | | 6,571 | 4,099 | 0.00002 | 62 |
| 109 | | 3,381 | 5,740 | 0.00004 | 170 |
| 112 | | 35,430 | 28,470 | 0.0004 | 80 |
| 114 | sorbitol dehydrogenase | 11,410 | 8,521 | 0.0005 | 75 |
| 120 | | 3,934 | 2,484 | 0.00009 | 63 |
| 149 | GSTP1 | 15,480 | 23,920 | 0.0003 | 155 |
| 156 | | 3,568 | 975 | 0.00002 | 27 |
| 166 | | 2,747 | 1,475 | 0.0004 | 54 |
| 169 | | 3,259 | 9,337 | 0.000004 | 286 |
| 176 | | 4,969 | 6,809 | 0.0008 | 137 |
| 196 | | 2,541 | 4,586 | 0.0004 | 180 |
| 201 | | 2,700 | 10,440 | 0.00004 | 387 |
| 206 | | 1,261 | 523 | 0.00008 | 41 |
| 212 | | 5,163 | 7,351 | 0.0006 | 142 |
| 234 | | 3,173 | 6,039 | 0.00005 | 190 |
| 235 | | 3,553 | 7,297 | 0.0001 | 205 |
| 244 | | 4,194 | 3,541 | 0.0008 | 84 |
| 246 | | 1,749 | 2,882 | 0.0005 | 165 |
| 263 | | 1,965 | 8,542 | 0.0009 | 435 |
| 272 | | 3,613 | 2,028 | 0.0001 | 56 |
| 296 | GSTP1 | 5,658 | 35,280 | 0.000005 | 624 |
| 300 | | 1,129 | 354 | 0.00005 | 31 |
| 313 | | 2,167 | 538 | 0.00003 | 25 |
| 319 | | 1,632 | 9,301 | 0.000007 | 570 |
| 338 | | 2,492 | 9,515 | 0.00001 | 382 |
| 339 | hsp70 | 1,007 | 1,320 | 0.02 | 131 |
| 340 | | 1,208 | 2,218 | 0.0005 | 184 |
| 353 | | 1,326 | 2,147 | 0.0004 | 162 |
| 383 | | 1,081 | 2,450 | 0.0005 | 227 |
| 410 | | 415 | 134 | 0.00005 | 32 |
| 414 | | 880 | 3,201 | 0.00003 | 364 |
| 448 | | 374 | 177 | 0.0002 | 47 |
| 464 | | 825 | 1,172 | 0.0003 | 142 |
| 490 | | 730 | 2,107 | 0.0005 | 289 |
| 493 | | 352 | 924 | 0.0007 | 262 |
| 509 | | 839 | 665 | 0.0005 | 79 |
| 537 | | 1,323 | 2,117 | 0.00004 | 160 |
| 641 | | 284 | 702 | 0.0003 | 247 |
| 705 | | 512 | 1,565 | 0.0004 | 306 |
| 735 | aldose reductase | - | 37,465 | NA | NA |
| 743 | | 374 | 1,812 | 0.0001 | 484 |
| 756 | GSTP1 | - | 4,666 | NA | NA |
| 761 | | 432 | 1,306 | 0.0002 | 302 |
| 762 | | 673 | 1,385 | 0.0006 | 206 |
| 804 | | - | 9,962 | NA | NA |
| 805 | | 8,549 | 50,950 | 0.0001 | 596 |
| 840 | GSTP1 | - | 946 | NA | NA |

[a]MSN = Master Spot Number; [b]PROB = probability, significance level

**Table 3. Rat kidney medulla cytosol proteins altered by lead exposure**

| [a]MSN | ID | Control Abundance | Lead Abundance | [b]PROB | % of Control |
|---|---|---|---|---|---|
| 26 | | 10,780 | 7,255 | 0.0006 | 67 |
| 54 | | 4,440 | 8,281 | 0.00009 | 187 |
| 66 | aflatoxin B1 aldehyde reductase | 47,716 | 91,227 | 0.00004 | 191 |
| 115 | | 13,601 | - | NA | NA |
| 137 | | 7,069 | 5,324 | 0.0002 | 75 |
| 153 | | 3,645 | 7,141 | 0.00005 | 196 |
| 165 | GSTP1 | 11,076 | 27,784 | 0.00006 | 251 |
| 170 | | 3,180 | 1,214 | 0.0003 | 38 |
| 207 | | 1,482 | 670 | 0.00007 | 45 |
| 237 | | 3,229 | 7,516 | 0.00005 | 233 |
| 245 | alpha-2 microglobulin | 4,014 | - | NA | NA |
| 503 | | 581 | 1,092 | 0.0005 | 188 |
| 587 | | 416 | 730 | 0.0005 | 175 |
| 651 | | 863 | 2,020 | 0.0001 | 234 |
| 703 | aldose reductase | 1,185 | 24,634 | 0.006 | 2079 |
| 748 | | - | 6,178 | NA | NA |

[a]MSN = Master Spot Number; [b]PROB = probability, significance level

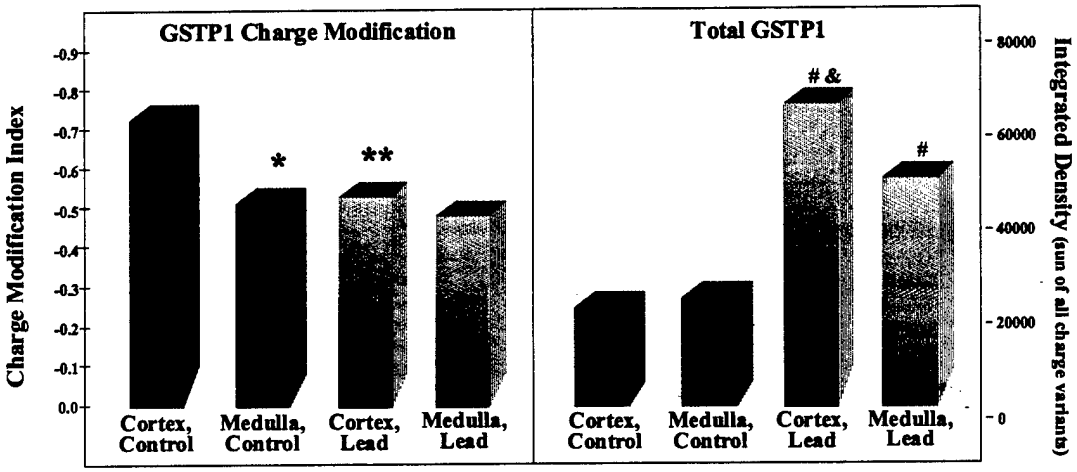


Figure 9. The effect of lead acetate on total GSTP1 abundance and GSTP1 CMI. * Mean (n=5) cortical GSTP1 is significantly different (P<.05) from medullary GSTP1 in controls. Only cortex GSTP1 CMI undergoes a significant decline with lead acetate exposure **(P<.05). #Total GSTP1 abundance increased by lead, &preferentially in cortex.

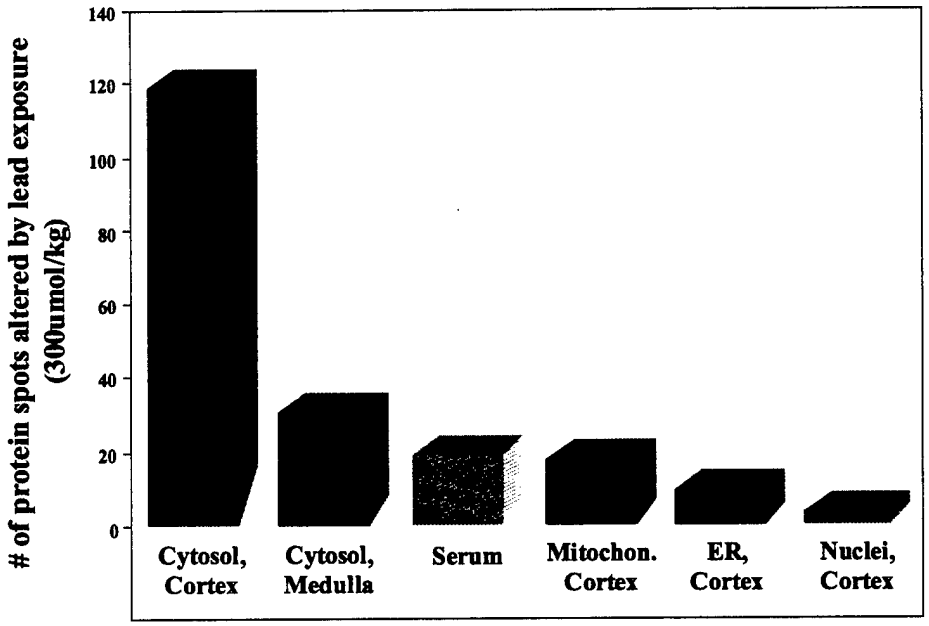


**Figure 10** Effect of Lead Exposure on protein abundance alterations in various cell fractions and serum

**Table 4. Identification of proteins in rat kidney cortex and medulla cytosols**

| IDENTIFICATION | CORTEX | | MEDULLA | | % Masses Matched | % Coverage | Sequence from Database |
|---|---|---|---|---|---|---|---|
| | MSN[a] | % of Control | MSN | % of Control | | | |
| actin, beta | 11 | 121 | 13 | 97 | - | - | HPGM[d] |
| actin, gamma | 19 | 9 | 20 | 107 | - | - | HPGM |
| aflatoxin B1 aldehyde reductase | 69 | 223 | 66 | 191 | 37 | 19 | (R)FYAFNPLAGGLLTGR(Y) |
| aldose reductase | 735 | NDC[b] | 703 | 2079 | 36 | 13 | (K)MPLVGLGTWKSSPGQVK(E) |
| alpha-2 microglobulin | 64 | 9 | 56 | 9 | 58 | 32 | (K)NGETFQLMVLYGR(T) |
| alpha-2 microglobulin | 85 | NDL[c] | 245 | NDL | 58 | 32 | (K)NGETFQLMVLYGR(T) |
| argininosuccinate synthase | 48 | 22 | 132 | 40 | 58 | 12 | (K)QHGIPIPVTPK(S) |
| calbindin | 36 | 60 | 135 | 71 | - | - | Ig[e] |
| calcineurin | 51 | 38 | 164 | 90 | - | - | Ig |
| calcineurin | 78 | 71 | 134 | 98 | - | - | Ig |
| GSTP1 | 149 | 155 | 142 | 152 | - | - | Ig |
| GSTP1 | 296 | 624 | 165 | 251 | - | - | Ig |
| GSTP1 | 756 | NDC | 751 | 194 | - | - | Ig |
| GSTP1 | 840 | NDC | ND | ND | - | - | Ig |
| hsc70 | 12 | 84 | 2 | 103 | - | - | Ig |
| hsc70 | 16 | 98 | 167 | 119 | - | - | Ig |
| hsp70 | 339 | 131 | 62 | 114 | - | - | Ig |
| hsp90 | 21 | 155 | 4 | 78 | - | - | Ig |
| hsp90 | 99 | 148 | 34 | 88 | - | - | Ig |
| sorbitol dehydrogenase | 114 | 75 | 225 | 82 | 54 | 26 | (R)LENYPIPELGPNDVLLK(M) |
| transferrin | 8 | 67 | 8 | 75 | 58 | 12 | (K)LPEGTTYEEYLGAEYLQAVGNIR(K) |
| transketolase | 15 | 131 | 23 | 111 | 56 | 18 | (R)TSRPENAIIYSNNEDFQVGQAK(V) |

*[a]MSN = Master Spot Number; [b]NDC = not detected in controls; [c]NDL = not detected in lead-exposed; [d]HPGM = identified by homologous position, gel matching;; [e]Ig = identified immunologically; Coverage refers to the amino acids in identified peptide sequences as a % of all amino acids in the protein.*

# Appendix C

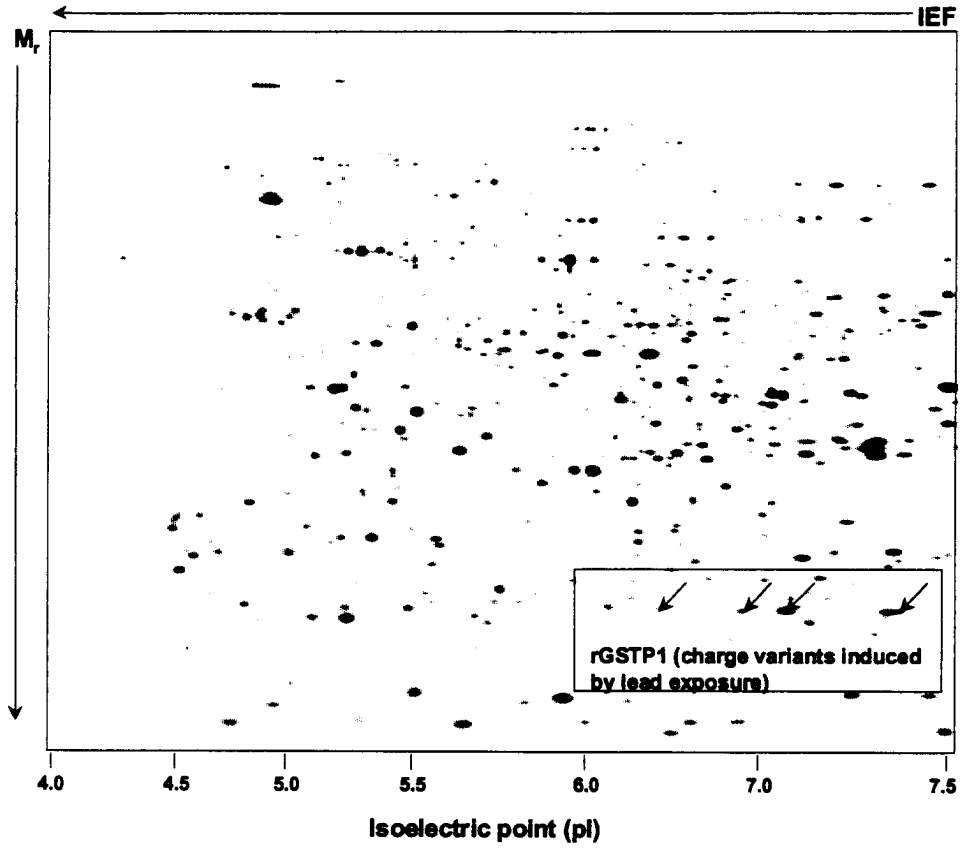


**Figure 11** 2-DE protein pattern of lead-exposed rat kidney cytosol. rGSTP1 was identified immunologically and is shown as native spot (pI=7.3) and three charge variants, ~pI 7.1, 6.9 and 6.3. In controls (see Figure 2a) rGSTP1 is resolved as only 2 spots (1 native spot and 1 charge variant; ~pI 7.3 and 7.1). The integrated densities of these spots were used to calculate total integrated density and charge modification index (CMI) in Figure 12, panel c.

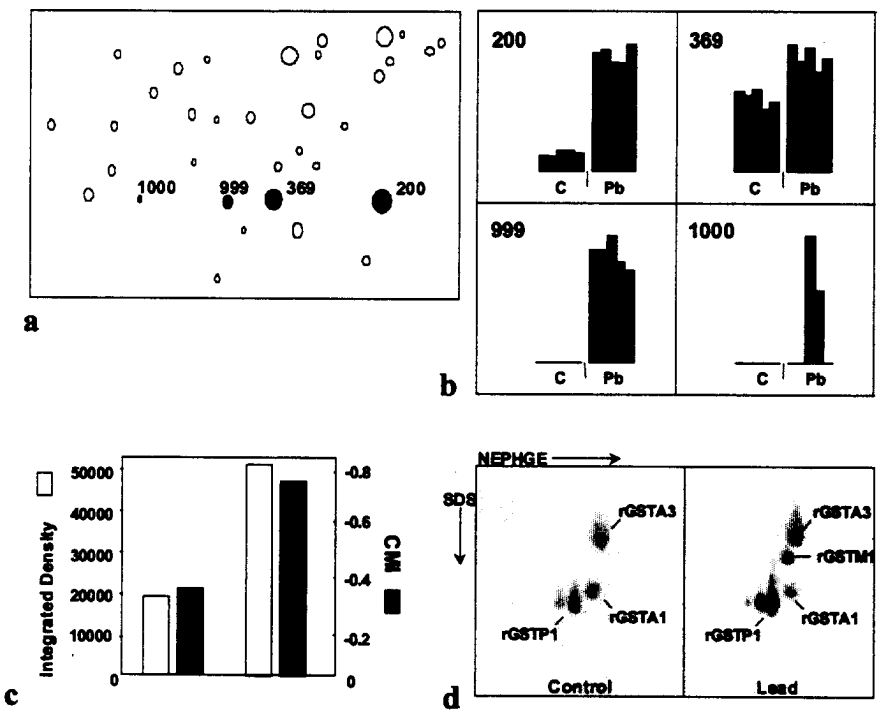


**Figure 12** A section of the computer-generated map containing the GSTP1 charge variants (blackened spots) and their master spot numbers (MSN). In controls, only 2 spots are resolved, the native, more basic form (MSN 200) and a single, more acidic charge variant (MSN 369). b. Bars indicating individual protein abundance (in each of the 5 samples, control and lead) illustrate that lead exposure increases MSN 200 and 369 abundance and causes the appearance of two additional acidic charge variants. All four spots were detected by the GSTP1 antibody. c. Bar graph illustrating a lead-induced increase in both rGSTP1 mean abundance □ (left axis) and mean CMI □ (right axis). CMI was calculated as described in the Methods. A leftward shift in protein charge as illustrated in panels a and b (and increased CMI) suggests lead-induced chemical modification of rGSTP1. d. Protein blots of kidney cytosol from control and lead-treated rats separated by NEPHGE-DALT electrophoresis. PVDF membranes were probed with anti-rGSTP1, anti-rGSTA1 and anti-rGSTM1 antibodies. The stained blots suggest a lead-induced increase in rGSTP1 and rGSTM1, as well as a slight leftward charge shift in rGSTP1 in agreement with the data observed via conventional 2-DE (panel a).

# Appendix D

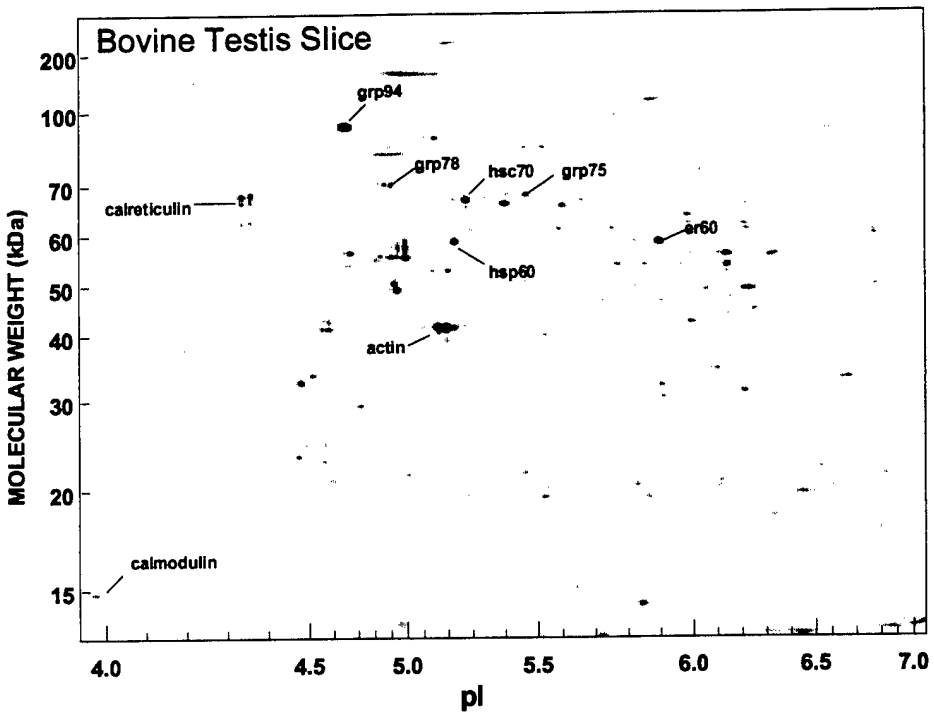


**Figure 13** Postscript rendition of a TIFF image representing the bovine testis slice master pattern. The axes of the map were determined by calculating MW or pI from the amino acid sequence of those spots identified in the pattern. Spots were identified as described previously [17].

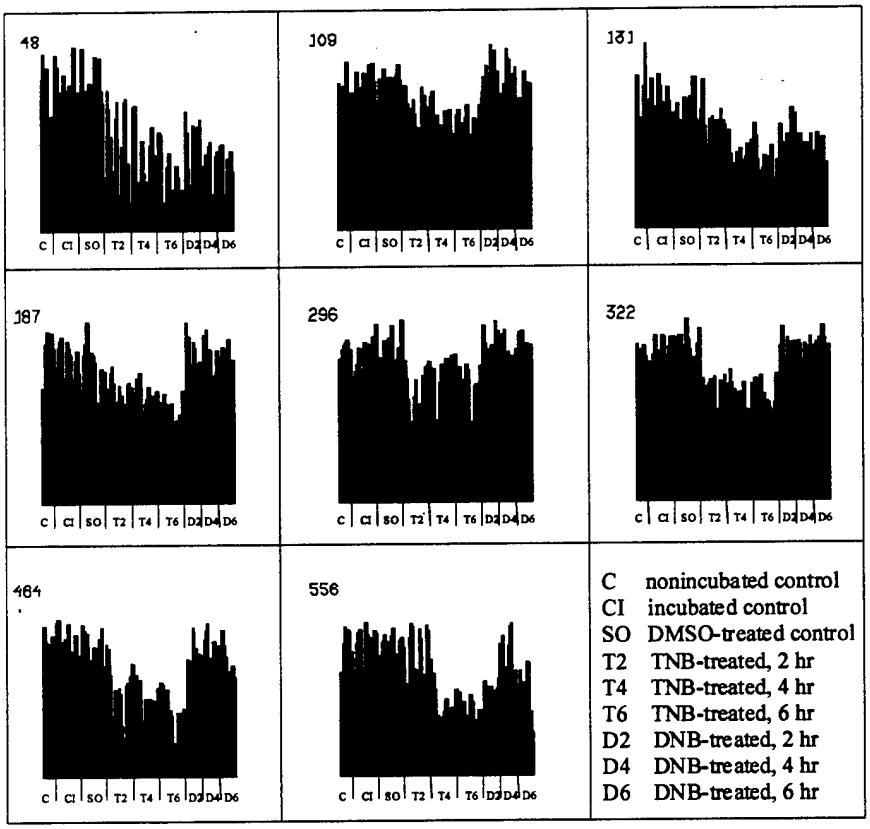


**Figure 14** Montage comparing the individual protein abundances (integrated spot volumes, processed as 2-D Gaussians) and the effect of incubation, TNB or DNB on them. Compared to controls, TNB increased ($P<.001$) the abundance of all proteins shown while DNB affected only MSN 161 and 451. Each bar represents the calculated product of a single spot density (or amplitude), 2 , sx, and sy and is thus shown with no units. As the legend indicates, bars are grouped by treatment. Within each treatment group, however, various doses are represented as follows: TNB, 100 µM first 3 bars, 500 µM middle 3 bars, 1 mM last 3 bars per time point; DNB, 100 µM first 2 bars, 500 µM middle 2 bars, 1 mM last 2 bars per time point.

# Appendix D (cont'd)

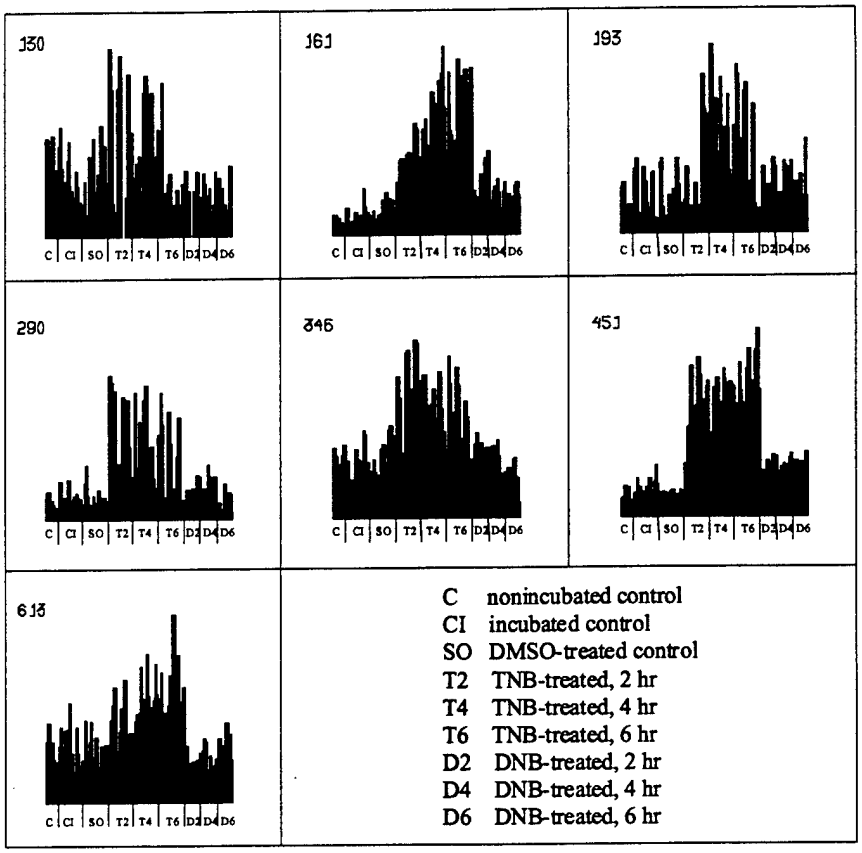


**Figure 15** Montage comparing the individual protein abundances (integrated spot volumes, processed as 2-D Gaussians) and the effect of incubation, TNB or DNB on them. Compared to controls, TNB decreased ($P<.001$) the abundance of all proteins shown, while DNB affected only MSN 48 and 131. Each bar represents the calculated product of a single spot density (or amplitude), 2 , sx, and sy and is thus shown with no units. As the legend indicates, bars are grouped by treatment. Within each treatment group, however, various doses are represented as follows: TNB, 100 □M first 3 bars, 500 □M middle 3 bars, 1 mM last 3 bars per time point; DNB, 100 □M first 2 bars, 500 □M middle 2 bars, 1 mM last 2 bars per time point.